International Journal on
"Technical and Physical Problems of Engineering"
(IJTPE)
Published by International Organization of IOTPE

ISSN 2077-3528
IJTPE Journal
www.iotpe.com
ijtpe@iotpe.com

December 2019 | Issue 41 | Volume 11 | Number 4 | Pages 1-10

COMPARISON AND EXPERIMENTAL VALIDATION OF THREE PHOTOVOLTAIC MODELS OF FOUR TECHNOLOGY TYPES

H. Idadoub [1] M. Kourchi [2] M. Ajaamoum [2] D. Yousfi [3] A. Rachdy [2]

1. Laboratory of Engineering Sciences and Energy Management, Higher School of Technology, Ibn Zohr University, Agadir, Morocco, hicham8ida@gmail.com
2. Electrical Engineering Department, Higher School of Technology, Ibn Zohr University, Agadir, Morocco, m.kourchi@uiz.ac.ma, m.ajaamoum@uiz.ac.ma, a.rachdy@uiz.ac.ma
3. Department of Electrical Engineering, National School of Applied Sciences, Mohammed First University, Oujda, Morocco, dr_yousfi@yahoo.com

Abstract- This work aims to develop models that best reproduce the electrical characteristics of photovoltaic panels (PV) of different technologies regardless of temperature and irradiance conditions. In this study, we examined two classes of PV panel models. The first class is derived from the theory of semiconductors taking into account the physical properties of PV cells. The second class uses a piecewise linear model obtained by linear interpolation between particular points of the *I*(*V*) characteristics of the PV modules. So as to identify the parameters of the proposed PV models, we operated an experimental database of the platform Green Energy Park of Benguerir (GEP). To determine and adjust the parameters, we used the robust optimization algorithm Levenberg-Marquardt and the adaptive inference system ANFIS.

Keywords: Photovoltaic Panel, Four-Parameter Model, Three-Parameter Model, Piecewise Linear Model, ANFIS.

I. INTRODUCTION

Solar energy is becoming an alternative technology of petroleum energy in the face of economic fluctuations, climate change and the progressive demand for energy in social life [1, 2]. The major problem of this new technology is its deficiency in conversion efficiency (30%) and the low competitiveness in the market because of the high cost of one-kilowatt hour.

In recent years, photovoltaic energy applications have largely developed under autonomous models, or connected to the network in several social, technical and economic sites. The conversion of solar energy to electrical energy that is given by photovoltaic systems (PVS) depends on the model estimating the equivalent circuit parameters, which are used to develop the photovoltaic emulators.

The photovoltaic emulator facilitates the experimental analysis of PVS, emulates the physical characteristics of solar and photovoltaic energy receivers. it is used to power systems under development and testing to evaluate its performance and behavior in various atmospheric conditions [3, 4]. It is based on a modeling of photovoltaic sources. However, the proper functioning of these emulators depends on the quality of the mathematical models used for the photovoltaic generators. The choice of these models directly affects the static and dynamic performance of the photovoltaic emulator.

This work aims to develop models that best reproduce the electrical characteristics of photovoltaic panels (PV) of different technologies regardless of temperature and irradiance conditions. These models will serve as a basis for real-time control of photovoltaic panel emulators.

In the first part, we present the two classes of the studied models of the PV panel. The first class is derived from the theory of semiconductors taking into account the physical properties of PV cells, and it is based on a single diode equivalent circuit [5]. The second class of models uses a piecewise linear model obtained by linear interpolation between particular points of the *I*(*V*) curves of the PV modules [6].

We then describe the methods for identifying the parameters of the proposed PV models, which require the use of an up-to-date experimental database representative of the meteorological conditions in Morocco. To do this, we operated an experimental database collected at Green Energy Park in Benguerir. For the determination and adjustment of the parameters, we used the robust optimization algorithm Levenberg-Marquardt and the adaptive inference system ANFIS [7].

Finally, we compare the experimental characteristics obtained for each of the four PV technologies with the simulation results of the proposed models, thus confirming their validity. The choice of best performance is based on criteria of simplicity, precision, and speed of execution.

II. STUDIED MODELS

Optimal operation of the emulators requires precise modeling of the PV source. Such modeling makes it possible to define the appearance of photovoltaic sources and to evaluate its behavior in the face of variable loading and meteorological conditions.

Figure 1 presents the two classes of models studied: The first class is derived from the theory of semiconductors; Which is based on the PV cell models with single exponential, namely the so-called "four-parameter model" and "three-parameter model". The identification of the parameters of these models uses three particular points of the electrical curve $I(V)$ of the photovoltaic module. this method reduces the measurement effort and precisely reconstructs the electrical appearance of the photovoltaic source [8].

The second class is presented as piecewise affine functions, which uses two other points of characteristic $I(V)$ in addition to the three points of the first class. The latter are used to determine the characteristic $I(V)$ by linear interpolation.

The five particular points used by piecewise affine functions are estimated by a system of equations based on irradiation and temperatures, which uses the LM algorithm (Levenberg-Marquardt) and ANFIS (the adaptive neuro-fuzzy inference system) for smoothing experimental measurements [5, 6, 7, 22 and 23].

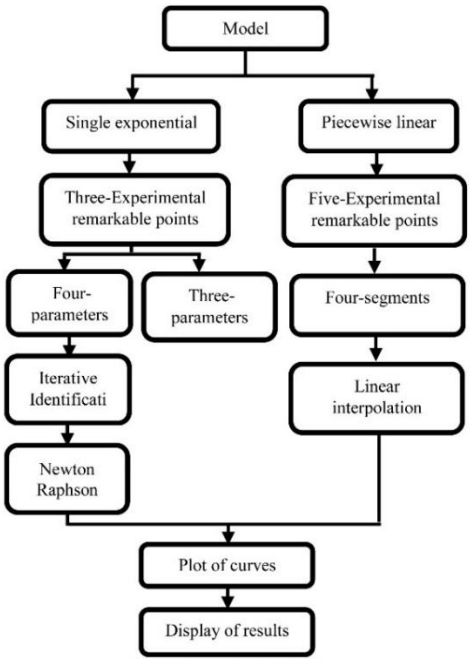

Figure 1. Model flowchart

A. Four-Parameter Model

The four-parameter model is represented in Figure 2 by the simplified equivalent electrical scheme of the PV module [7, 8].

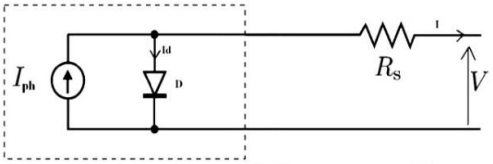

Figure 2. Equivalent diagram of the four-parameter model

The current discharged by the PV panel, follows the Equation (1):

$$I = I_{ph} - I_0\left[\exp\left(\frac{V+R_s\,I}{AV_t}\right)-1\right] \tag{1}$$

Since model (1) is an implicit nonlinear equation, only iterative methods can solve it. In our case, we use the Newton-Raphson (N-R) method, which has a fast rate of convergence and is one of the most used methods for solving nonlinear equations. Thus, the current I generated by the photovoltaic panel can be calculated iteratively according to Equation (3).

$$I_{k+1} = I_k - \frac{I_{ph} - I_0\left[\exp\left(\frac{V+R_s\,I_k}{A\,V_t}\right)-1\right] - I_k}{-I_0\,\frac{R_s}{A\,V_t}\exp\left(\frac{V+R_s\,I_k}{A\,V_t}\right)-1} \tag{2}$$

Here is Equation (1) in a simple form:

$$I = I_{ph} - \exp\left(\left(V+R_s\,I\right)K_1 + K_2\right) + \exp(K_2) \tag{3}$$

where

$$\begin{cases} \dfrac{1}{AV_t} = K_1 \\ I_0 = e^{K_2} \end{cases}$$

The behavior of the PV source can be studied if the four parameters $R_s, K_1, K_2,$ and I_{ph} are identified. The above-mentioned parameters can be obtained by first calculating their initial values by the following system of equations:

$$\begin{cases} K_1 = \dfrac{\dfrac{I_{mp}}{I_{ph}-I_{mp}} + \log\left(1-\dfrac{I_{mp}}{I_{ph}}\right)}{2V_{mp}-V_{oc}} \\ R_s = \dfrac{V_{mp} - \dfrac{I_{mp}}{\left(I_{ph}-I_{mp}\right)K_1}}{I_{mp}} \\ K_2 = \log\left(I_{ph}\right) - V_{oc}\,K_1 \\ I_{ph} = I_{sc} + \exp\left(R_s\,I_{sc}\,K_1 + K_2\right) \end{cases} \tag{4}$$

The resolution of the system of nonlinear equation in Equation (4) will follow the steps mentioned:

1) Initial value for $I_{ph} = I_{sc}$;

2) Calculate K_1 by replacing I_{ph} in the first system Eequation (4);

3) Calculate R_s and K_2 respectively by replacing I_{ph} and K_1 in the second and third system Equation (4);

4) Calculate $I_{ph\,new}$ the new value of I_{ph} by replacing K_1, K_2 and R_s in the fourth system Equation (4);

Iterations from 2 to 4 are stopped by the variation $\Delta I_{ph} = (I_{ph\,new} - I_{ph})$ is below a threshold. Generally, the convergence is achieved in some iterations.

B. Three-Parameters Model

This model enables the calculation of the electrical characteristic $I(V)$ of the PV panel regardless of the irradiance and temperature conditions using Equation (5):

$$I = I_{sc}\left\{1 - C_1\left(\exp\left(C_2\, V^m\right) - 1\right)\right\} \quad (5)$$

The three unknown parameters C_1, C_2, and m are determined according to I_{mp}, V_{mp}, V_{oc}, and I_{sc} for a given solar irradiance and temperature. The coefficient C_1 is fixed at 0.01175 [7] by manufacturers, while the coefficients m and C_2 are identified according to Eequations (6) and (7):

$$m = \frac{\ln\left(\frac{C_3}{C_4}\right)}{\ln\left(\frac{V_{mp}}{V_{oc}}\right)} \quad (6)$$

$$K_2 = \frac{C_4}{V_{co}^m} \quad (7)$$

with:

$$C_3 = \ln\left(\frac{I_{sc}\left(1+C_1\right) - I_{mp}}{C_1 I_{sc}}\right) \text{ and } C_4 = \ln\left(\frac{1+C_1}{C_1}\right)$$

C. Piecewise Linear Model: Four-Segment

The objective here is to draw the curve *I(V)* consisting of segmented straight lines, with a number of points given at the start. The choice of these starting points is an important element for the elaboration of the piecewise linear model. These points are determined on the basis of *G* and *T* and can then be used to calculate the other points of characteristic *I*(*V*) by linear interpolation [8]. To improve accuracy, we selected five points:

$$(0, I_{sc}),\ \left(\frac{V_{oc}}{2}, I_1\right),\ \left(V_{mp}\, I_{mp}\right),$$

$$\left(\frac{V_{oc}+V_{mp}}{2},\ I_2\right),\ \left(V_{oc},\ 0\right)$$

As a result, we will have five points and four lines Figure 3.

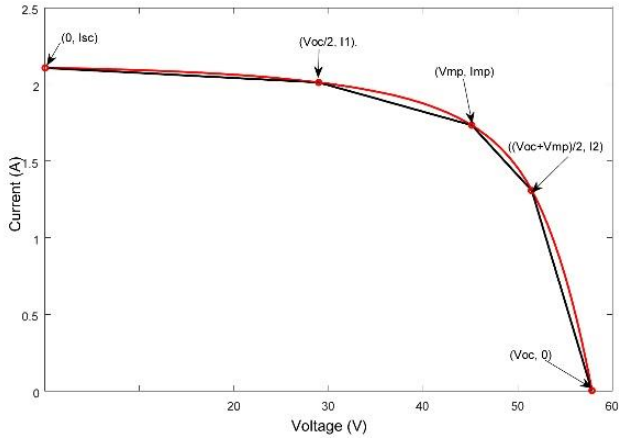

Figure 3. Four-segment interpolation model

The four equations representing the four lines are given by:

$$\begin{cases} I = I_2 - I_2\dfrac{V - V_2}{V_{OC} - V_2} & ;\quad V_2 \le V \le V_{oc} \\ I = I_{mp} + \left(I_2 - I_{mp}\right)\left(\dfrac{V - V_{mp}}{V_2 - V_{mp}}\right) & ;\quad V_{mp} \le V \le V_2 \\ I = I_1 + \left(I_{mp} - I_1\right)\left(\dfrac{V - V_1}{V_{mp} - V_1}\right) & ;\quad V_1 \le V \le V_{mp} \\ I = I_{sc} + \left(I_1 - I_{sc}\right)\left(\dfrac{V}{V_1}\right) & ;\quad 0 \le V \le V_1 \end{cases} \quad (8)$$

where

$$V_1 = \left(\frac{V_{oc}}{2}\right), V_2 = \left(\frac{V_{oc}+V_{mp}}{2}\right)$$

D. Identification of Five *I*(*V*) Points

To identify the five particular points of characteristic *I*(*V*), we solved the estimation problem using a system of equations obtained by adjusting the experimental data. The calculation of V_{oc} and V_{mp} voltages was established by the neuro-fuzzy system ANFIS, which does not require a particular form of modeling given the difficulties of modeling encountered by simple parametric equations.

D.1. Identification of Currents

The model is based on three particular points I_{sc}, (I_{mp}, V_{mp}) and V_{oc} calculated by adjusted equations:

$$\begin{cases} I_{sc} = I_{scn}\left(a_1 + b_1\dfrac{G}{G_n} + c_1\left(T - T_n\right)\right) \\ I_{mp} = I_{mpn}\left(a_2 + b_2\dfrac{G}{G_n} + c_2\left(T - T_n\right)\right) \\ I_1 = I_{scn}\left(a_3 + b_3\dfrac{G}{G_n} + c_3\left(T - T_n\right)\right) \\ I_2 = I_{scn}\left(a_4 + b_4\dfrac{G}{G_n} + c_4\left(T - T_n\right)\right) \end{cases} \quad (9)$$

The Levenberg-Marquardt algorithm determines the coefficients a_i, b_i, c_i. This is a specific optimization method for the minimization of non-linear least squares problems, and it is very often used in parameter identification. It makes it possible to adjust the coefficients a_i, b_i, c_i in order to minimize the difference between the measured and calculated points.

To evaluate the I_{sc} and I_{mp} currents predicted by the model (9), we compared them with the models using the manufacturer's data. The data sheets provide temperature coefficients at maximum power, short-circuit and open-circuit points. With the help of the temperature coefficients, the currents I_{sc} and I_{mp} can be expressed by the temperature and the radiation according to the Equation (10).

$$\begin{cases} I_{sc} = I_{scn}\dfrac{G}{G_n} + K_i\left(T - T_n\right) \\ I_{mp} = I_{mpn}\dfrac{G}{G_n} + K_{mp}\left(T - T_n\right) \end{cases} \quad (10)$$

D.2. Identification of V_{oc} and V_{mp}

For the identification of V_{oc} and V_{mp}, we opted for the neuro-fuzzy approach. The neuro-fuzzy systems that combine fuzzy logic and neural networks have proven their effectiveness in a variety of industrial problems. They are useful for the identification of non-linear, complex systems, which are difficult to model.

Indeed, the experimental voltages V_{oc} and V_{mp} resisted our attempts to model by simple parametric equations. Therefore, we chose to use the neuro-fuzzy adaptive inference systems ANFIS, which do not require taking on a particular form of modeling. It is a five-layer multilayer Perceptron neuron network for which each layer corresponds to the completion of a step of a Takagi Sugeno-type fuzzy inference system (FIS) [13].

A Matlab code is developed for the generation of the ANFIS model according to the flowchart in Figure 4.

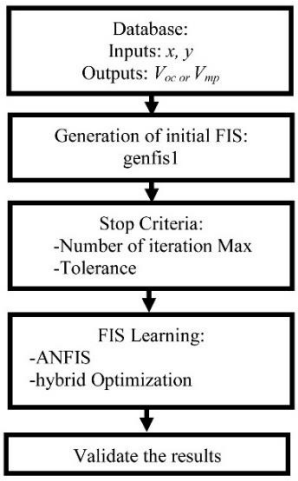

Figure 4. The flowchart of the code developed

After several learning tests, we arrived at the architecture of the simplest and most efficient ANFIS model illustrated in Figure 5.

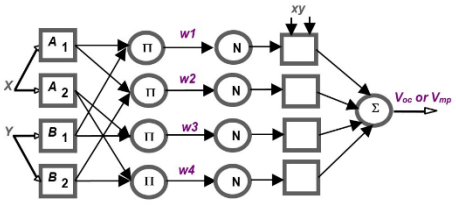

Figure 5. ANFIS architecture used

It has two inputs and a polynomial output of order 1. Each entry is represented by two fuzzy sets of Gaussian type. The inputs x and y are expressed in terms of the radiation G and the temperature T of the PV module according to the equation system (11).

$$\begin{cases} x = \dfrac{G}{G_n} + T - T_n \\ y = \left(T + 273.15\right)\log\left(\dfrac{G}{\left(T + 273.15\right)G_n}\right) \end{cases} \quad (11)$$

To evaluate the V_{oc} and V_{mp} voltages predicted by the ANFIS model, we compared its results with those calculated by the proposed model (12) obtained by smoothing the experimental measurements.

$$\begin{cases} V_{oc} = V_{ocn} + a_4 V_t \log\left(\dfrac{G}{G_n}\right) + b_4\left(T - T_n\right) \\ V_{mp} = V_{mpn} + a_5 V_t \log\left(\dfrac{G}{G_n}\right) + b_5\left(T - T_n\right) \end{cases} \quad (12)$$

III. RESULTS AND EXPERIMENTAL VALIDATION

A. Development Tools

The experimental bench used to characterize the parameters of the panels is located in Green Energy Park of Benguerir-Morocco [11]. It is comprised of an active charge, a temperature sensor (pt 1000), a sun sensor (hemispherical solar radiation), and a data acquisition server (PV Analyser - SQL Connect Center) [18].

Figure 6. GEP measuring station

To simulate the different models, we chose the Matlab 2016a environment. It is complete, open, and expandable for calculation and visualization. The PV technologies studied are of four types. Their technical specifications are grouped in Table 1.

Table 1. Electrical parameters of the solar modules used

PV Module	Amorphous [21]	CIS [23]	Mono-Si [20]	Cdte [22]
$P_{\max}(W)$	135	120	190	77.5
N_s	--	--	72	--
$I_{sc}(A)$	3.41	3.22	5.52	1.92
$I_{mp}(A)$	2.88	2.81	5.18	1.68
$V_{mp}(V)$	47	42.8	36.8	46.6
$V_{oc}(V)$	61.3	58.3	45.1	62
$K_i(\%/°C)$	0.07	0.1 mA/°C	0.05	0.02 %/°K
$K_v(\%/°C)$	-0.3	-170 mV/ °C	-0.35	-0.24 %/°K
$K_{mp}(\%/°C)$	-0.24	-0.39	-0.45	-0.25 %/°K
$NOCT(°C)$	--	--	46	45

B. Evaluation Criteria

To assess the precision of the estimated parameters and the smoothing quality, we calculated the *Rd* and the *RMSE* respectively coefficient of determination and mean square error for each technology studied [14, 15].

The coefficient of determination is an indicator of the quality of a linear, single or multiple regression. Its value is taken between zero and one. The reason why the coefficient of determination R_d is a better measure is due to the fact that it tells us about the effect of the independent variable on the dependent variable. It is calculated by taking into account the parameters of the model, according to the expression (13):

$$R_d = 1 - \frac{\sum_{i=1}^{N}\left(G_{mes}(i) - G(i)\right)^2}{\sum_{i=1}^{N}\left(G_{mes}(i) - \overline{G_{mes}}\right)^2} \quad (13)$$

where, $\overline{G}_{mes} = \frac{\sum_{i=1}^{N} G_{mes}(i)}{N}$ is the arithmetic mean of the measured magnitude *G*.

The *RMSE* mean square error also known as the *RMSD* (Root Mean Square Deviation) is according to the formula of Equation (14) [16].

$$RMSE = \sqrt{\sum_{i=1}^{N} \frac{\left(G_{i\ mes} - G_{i\ cal}\right)^2}{N}} \quad (14)$$

In order to estimate the speed of execution of each of the models studied, we evaluated the average calculation time, t_{CPU} necessary for the calculation of characteristics *I*(*V*) of all the measures considered. For the processing performed during our investigations, we used a PC-type computer with the Intel(R) Core (TM) i5-4310U CPU @ 2.00GHz processor, 2601 MHz, 2 core(s), 4 logic processor(s), with a RAM memory of 4 GB capacity.

C. Results of Identification of Five Points Curve *I*(*V*)

C.1. Current Identification Results

The identified values of the coefficients a_i, b_i, c_i of Equation (9) for the four technologies are summarized in Table 2. Figures 7 shows a comparison between the experimental values and the values predicted by the system of Equations (9) of the four technologies studied.

Table 2. Identified parameters

Parameter	Coef.	Amorphous	CIS	Mono-Si	CdTe
I_{sc}	a_1	-0.0053	-0.0043	0.0061	-0.0009
	b_1	0.9768	0.9731	1.0247	0.9800
	c_1	0.0002	-0.0003	0.0002	0.0000
I_{mp}	a_2	-0.0060	-0.0014	0.0079	-0.0370
	b_2	0.9712	0.9591	1.0161	0.9226
	c_2	0.0005	-0.0002	0.0000	-0.0018
I_1	a_3	-0.0052	-0.0039	0.0020	-0.0291
	b_3	0.9430	0.9487	1.0261	0.9242
	c_3	0.0004	-0.0003	0.0000	-0.0013
I_2	a_3	0.0064	0.0236	0.0342	-0.0026
	b_3	0.5907	0.5102	0.6671	0.4912
	c_3	0.0003	0.0004	-0.0003	-0.0006

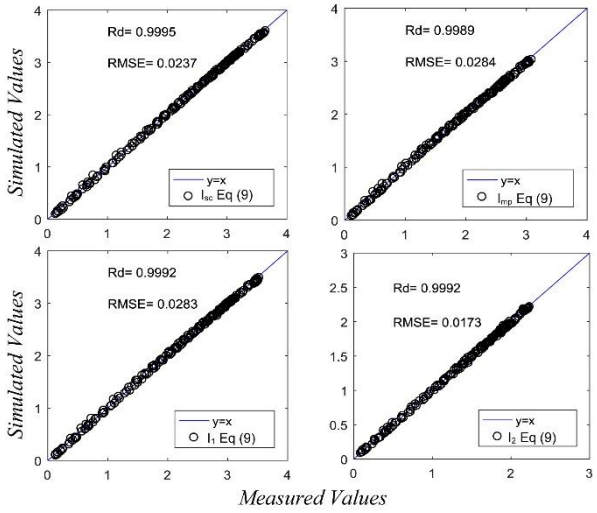

Figure 7. Comparison of simulated and measured currents for Amorphous technology

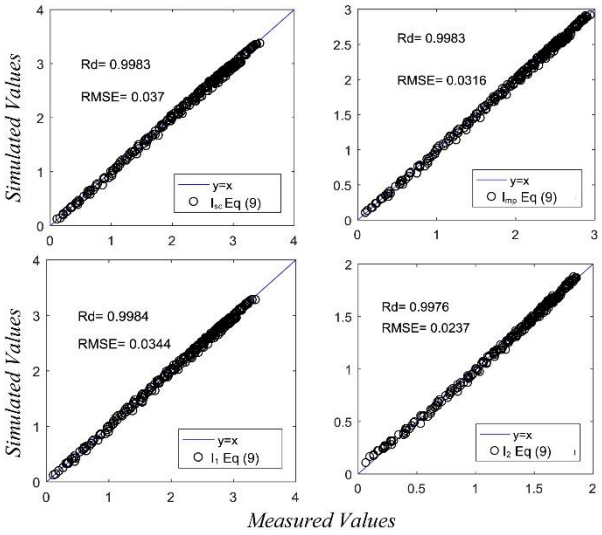

Figure 8. Comparison of simulated and measured currents for CIS technology

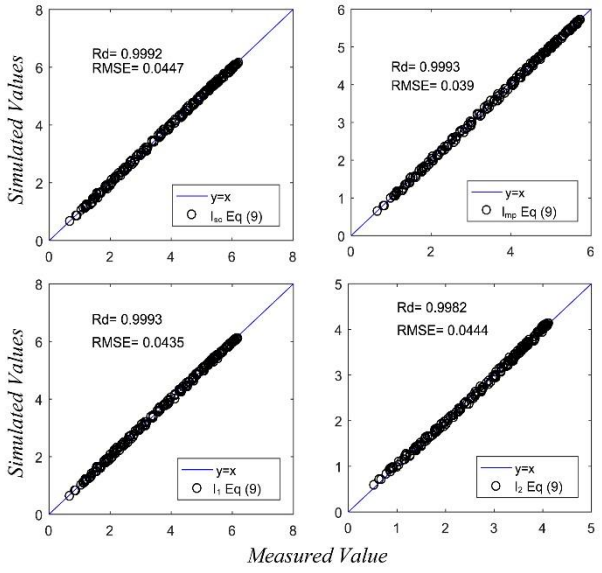

Figure 9. Comparison of simulated and measured currents for Mono technology

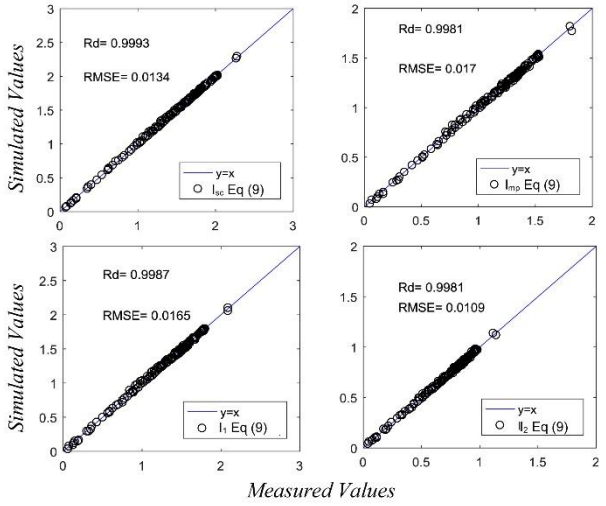

Figure 10. Comparison of simulated and measured currents for CdTe technology

The calculated values of R_d and *RMSE* for each parameter are grouped in Table 3. We proceeded to compare the proposed model (9) with the model (10) using the manufacturer's data.

Table 3. Comparison of simulated and measured currents

Technology	Par.	Model (9)		Model (10)	
		R_d	*RMSE*	R_d	*RMSE*
Amorphous	I_{sc}	0.9995	0.0237	0.9914	0.0956
	I_{mp}	0.9989	0.0284	0.9950	0.0619
	I_1	0.9992	0.0283	--	--
	I_2	0.9992	0.0173	--	--
CIS	I_{sc}	0.9983	0.0370	0.9882	0.0972
	I_{mp}	0.9983	0.0316	0.9967	0.0443
	I_1	0.9984	0.0344	--	--
	I_2	0.9976	0.0237	--	--
Mono-Si	I_{sc}	0.9992	0.0447	0.9936	0.1283
	I_{mp}	0.9993	0.0390	0.9617	0.2904
	I_1	0.9993	0.0435	--	--
	I_2	0.9982	0.0444	--	--
CdTe	I_{sc}	0.9993	0.0134	0.9926	0.0439
	I_{mp}	0.9981	0.0170	0.8453	0.1546
	I_1	0.9987	0.0165	--	--
	I_2	0.9981	0.0109	--	--

The results obtained show that the system of Equations (9) is more precise for the four technologies than the system (10) using the manufacturer's data. This demonstrates the suitability and validity of the chosen mathematical model.

C.2. Results of Identification of Tensions V_{oc} and V_{mp}

In Figure 8, the values predicted by the ANFIS model and the model (12) are compared with the experimental values corresponding to the four technologies studied.

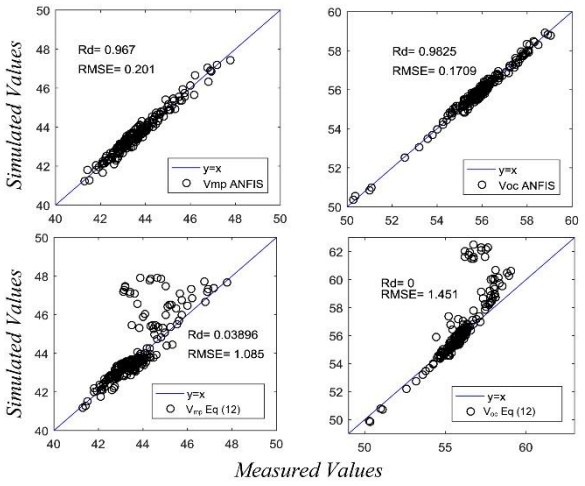

Figure 11. Comparison of simulated and measured voltages for amorphous technology

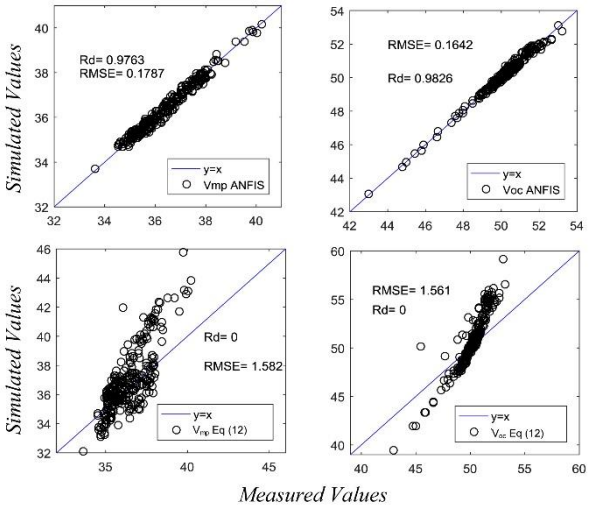

Figure 12. Comparison of simulated and measured voltages for CIS Technology

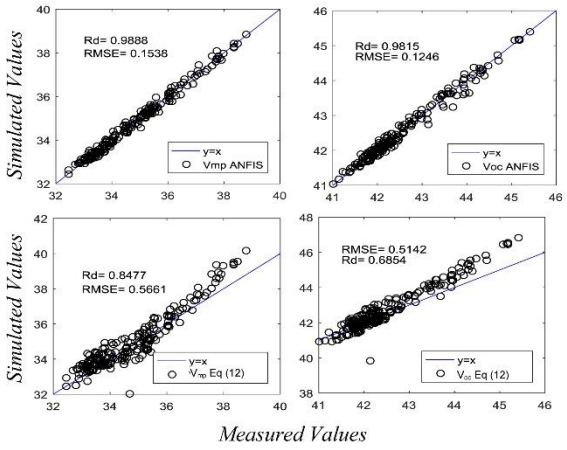

Figure 13. Comparison of simulated and measured voltages for Mono technology

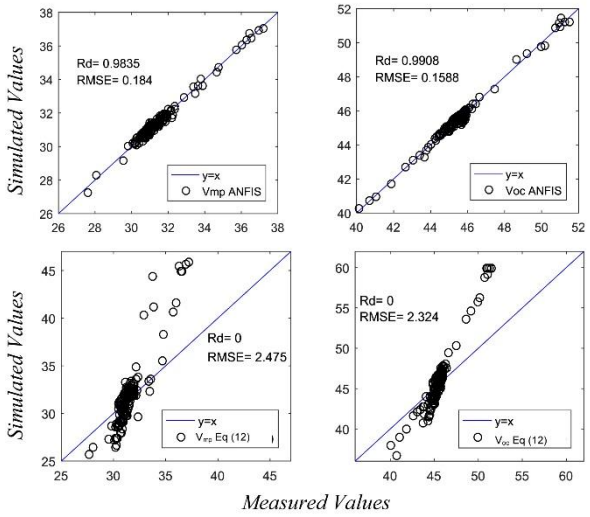

Figure 14. Comparison of simulated and measured voltages for CdTe technology

Table 4 summarizes the calculated values of the R_d and the *RMSE* corresponding to the calculation of V_{oc} and V_{mp} voltages by the model ANFIS and model (12).

Table 4. Comparison of model ANFIS and model 12

Technology	Par.	Model ANFIS		Model (12)	
		R_d	*RMSE*	R_d	*RMSE*
Amorphous	V_{oc}	0.9825	0.1709	0	1.4509
	V_{mp}	0.9670	0.2010	0.0390	1.0854
CIS	V_{oc}	0.9826	0.1642	0	1.5613
	V_{mp}	0.9763	0.1787	0	1.5823
Mono-Si	V_{oc}	0.9815	0.1246	0.6854	0.5142
	V_{mp}	0.9888	0.1538	0.8477	0.5661
CdTe	V_{oc}	0.9908	0.1588	0	2.3241
	V_{mp}	0.9835	0.1840	0	2.4752

The results are satisfactory for both V_{oc} and V_{mp} voltages. The different comparisons allow confirming the performance and the correct concordance between measurement and modeling by the ANFIS neuro-fuzzy system. This shows us the efficiency and the ability to identify this model.

D. Characteristic *I*(*V*): Results Calculation

This section presents some results for Comparing the experimental characteristics *I*(*V*) and those obtained by the proposed models. For all measurement samples, model performance is summarized in Table 5 for the four technologies.

D.1. Four Parameters Model

Figure 15 shows an example of four-parameter model application results for the four technologies studied. *I*(*V*) characteristics are recorded for various values of *G* and *T*. We found that the simulated values are consistent with the experimental measurements.

D.2. Three Parameters Model

Figure 16 shows an example of 3-parameter model application results for the four technologies studied. *I*(*V*) characteristics are recorded for variant values of *G* and *T*. We find that the simulated values are consistent with the experimental measurements.

D.3. Piecewise Affine Model

Figure 11 shows an example of the application results of the piecewise affine model for the four technologies studied. The *I*(*V*) characteristics are recorded for different values of *G* and *T*. A good coincidence is found between simulated values and experimental measurements.

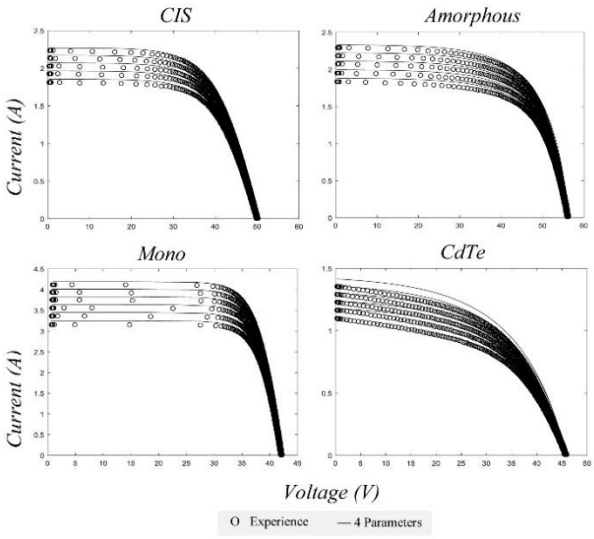

Figure 15. Experimental and simulated *I*(*V*) characteristics of the four-parameter model

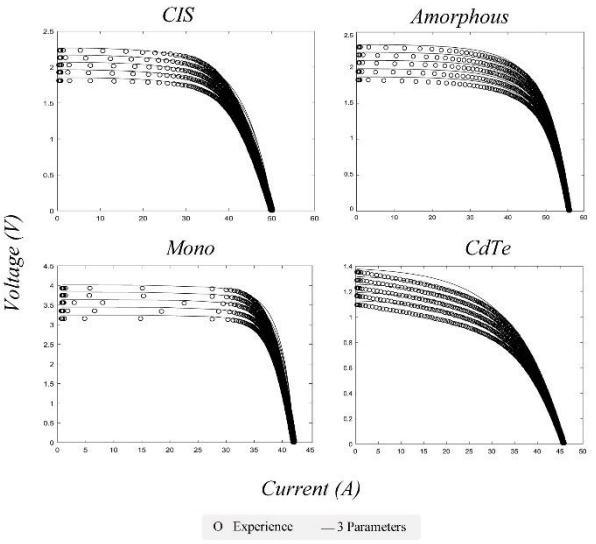

Figure 16. Experimental and simulated *I*(*V*) characteristics by the three-parameter model (5-7)

D.4. Summary Results

For the completely experimental database, the results for comparing the performance of the models used in this study are grouped in Table 5.

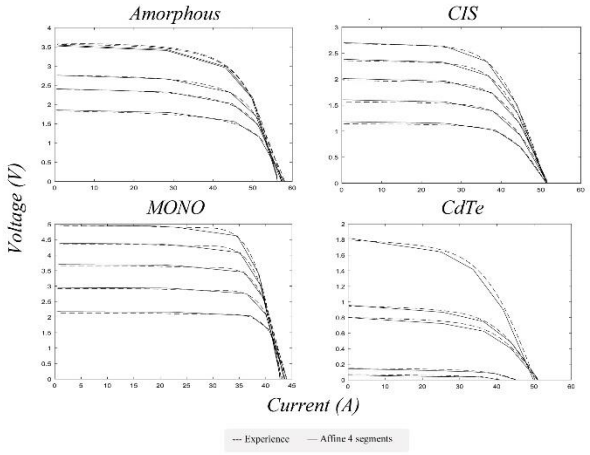

Figure 11. Experimental and simulated *I*(*V*) characteristics of the 4-segment affine model

Table 5. Summary of performance and calculation time t_{CPU}

Technology	Critria	Four-parameter model	Three-parameter model	Four-segment affine model
SHARP NS-F135G5 Amorphous	R_d	0.9884	0.9977	0.9864
	RMSE	0.0993	0.0444	0.1076
	t_{CPU}(s)	0.0381	0.0375	0.0398
Power Max STRONG 120 CIS	R_d	0.9984	0.9651	0.9948
	RMSE	0.0347	0.1627	0.0626
	t_{CPU}(s)	0.0351	0.0413	0.0369
TSM-DC01A Mono-Si	R_d	0.9960	0.9233	0.9834
	RMSE	0.0964	0.4244	0.1974
	t_{CPU}(s)	0.0384	0.0395	0.0372
Calyxo Cx3 Cdte	R_d	0.9746	0.9971	0.9966
	RMSE	0.0845	0.0283	0.0308
	t_{CPU}(s)	0.0368	0.0444	0.0366

Table 6. Average criteria for the four technologies

Average criteria	Four-parameter model	Three-parameter model	Four-segments affine model
R_d	0.9894	0.9708	0.9903
RMSE	0.0787	0.165	0.0996
t_{CPU}(s)	0.0371	0.041	0.0376

To evaluate the performances of the studied models, we calculated the average values of the different criteria in Table 6. The analysis of the results in Table 6 shows that there is a small difference between the four-segment model and four-parameter model on a precision level (about 0.99). However, the four-parameter model adds more the squared error (0.0787) and speed of execution, which attained 0.03908s.

IV. CONCLUSION

This article focused on experimental validation applied to PV panel models. In this study, we searched for the model that best reproduces the characteristics of the PV panels of four technologies: Monocrystalline silicon (TSM-DC01A), microcrystalline amorphous (SHARP NS-F135G5), CIS (Power Max STRONG 120) and the CdTe (Calyxo Cx3 cdte).

The problem of estimating the currents I_{sc}, I_{mp}, I_1, I_2 for the four technologies is solved by using a system of equations obtained by adjusting the experimental data. For the calculation of V_{oc} and V_{mp} voltages, we have successfully used the ANFIS neuro-fuzzy system. The study results show that the models proposed are more precise than those which use data from the PV modules data sheet.

Following the comparisons made, we found that a very good compromise of precision and speed of execution is obtained by the implicit model with four-parameter.

NOMENCLATURES

N_s : Number of cells in series

I_{ph} : Photocurrent generated (A)

R_s : Series resistance (Ω)

I_0 : Reverse diode saturation current (A)

I_{sc} : Short circuit current (A)

V_{oc} : Open circuit voltage (V)

k: Boltzmann Constant (1.381×10^{-23} J/K)

q : Electron charge (1.6×10^{-19} C)

$V = N_s k_t / q$: Thermodynamic potential of connected cells in series

I_{mp} : Maximum power current (A)

V_{mp} : Voltage at maximum power (V)

K_{mp} : Temperature coefficient of the maximum power point

K_v : Open circuit voltage temperature coefficient

K_i : Temperature coefficient of the short-circuit current $\left(\text{mA}/^{\circ}\text{C}\right)$

T: Solar Temperature $\left(^{\circ}\text{C}\right)$

G: Solar Irradiance in $\left(\text{W/m}^2\right)$

$P_{\max}$: Maximum panel power (W)

ACKNOWLEDGEMENTS

This article is the result of PV-EMUL project sponsored by the Research Institute of Solar Energy and New Energies "IRESEN" as part of the call for projects InnoProjets2015. In particular, we would like to thank the IRESEN Director and staff for their continued support of this project from very beginning. We would also like to thank entire PVS team at Green Energy Park "GEP" for help and time given for development of an experimental database of existing photovoltaic modules at GEP.

REFERENCES

[1] L. Peng, Y. Sun, Z. Meng, "An Improved Model and Parameters Extraction for Photovoltaic Cells Using only Three State Points at Standard Test Condition", Journal of Power Sources, Vol. 248, pp. 621-631, Feb. 2014.

[2] V. Khanna, B.K. Das, D. Bisht, Vandana, P.K. Singh, "A Three-Diode Model for Industrial Solar Cells and Estimation of Solar Cell Parameters Using PSO Algorithm", Renewable Energy, Vol. 78, pp. 105-113, Jun. 2015.

[3] M.Sh. Uddin, "Performance Based Analysis of Solar PV Emulators: A Review", International Conference on Computational and Characterization Techniques in Engineering & Sciences (CCTES) Integral University, Lucknow, India, 14-15 Sep. 2018.

[4] P.J. Binduhewa, M. Barnes, "Photovoltaic Emulator", 8th International Conference on Industrial and Information Systems, pp. 519-524 University of Peradeniya Sri Lanka, 18-20 Dec. 2013.

[5] T.R. Ayodele, A.S.O. Ogunjuyigbe, E.E. Ekoh, "Evaluation of Numerical Algorithms Used in Extracting the Parameters of a Single-Diode Photovoltaic Model", Sustainable Energy Technologies and Assessments, Vol. 13, pp. 51-59, 2016.

[6] B. Zina, B.H. Mouna, S. Lassaad, "Photovoltaic Cell Mathematical Modeling", International Journal of Engineering Research & Technology (IJERT), Vol. 6, Issue 6, Jun. 2017.

[7] M.U. Siddiqui, M. Abido, "Parameter Estimation for Five- and Seven-Parameter Photovoltaic Electrical Models Using Evolutionary Algorithms", Applied Soft Computing, Vol. 13, pp. 4608-4621, 2013.

[8] M.C. Di Piazza, G. Vitale, "Photovoltaic Sources", Springer Nature, 2013.

[9] D. Meekhun, "Realization of a System for Converting and Managing the Energy of a Photovoltaic System for the Supply of Autonomous Wireless Sensor Networks for the Aeronautical Application", PhD thesis, University of Toulouse, France, 2011.

[10] M. Ajaamoum, M. Kourchi, B. Bouachrine, A. Ihlal, L. Bouhouch, "Photovoltaic Panel Emulators, Design and Implementation Using Rapid Prototyping Technique", International Review of Electrical Engineering (IREE), Vol. 9, No. 5, Sept.-Oct. 2014.

[11] http://www.greenenergypark.ma/.

[12] R. Khezzar, M. Zereg, A. Khezzar, "Modeling Improvement of the Four Parameter Model for Photovoltaic Modules", Solar Energy Vol. 110, pp. 452-462, Dec. 2014.

[13] Y.J. Wang P.C. Hsu, "Modeling of Solar Cells and Modules Using Piecewise Linear Parallel Branches", IET Renewable Power Generation, Vol. 5, Issue 3, pp. 215-222, May 2011.

[14] E.H.M. Ndiaye, A. Ndiaye, M.A. Tankari, G. Lefebvre, "Adaptive Neuro-Fuzzy Inference System Application for the Identification of a Photovoltaic System and the Forecasting of Its Maximum Power Point", 7th International Conference on Renewable Energy Research and Applications (ICRERA), Paris, France, 14-17 Oct. 2018.

[15] M. Hatti, "Artificial Intelligence in Renewable Energetic Systems", Springer Science and Business Media LLC, 2018.

[16] R. Eke, H. Demircan, "Performance Analysis of a Multi Crystalline Si Photovoltaic Module under Mugla Climatic Conditions in Turkey", Energy Conversion and Management, Vol. 65, pp. 580-586, 2013.

[17] Technical Sheet: SOL Connect Multiscan and MultiIO, Papendorf Software Engineering GmbH, 12 June 2013.

[18] Technical Sheet of TSM-DC01A- Trina Solar Limited-Leutschenbachstr.45, 8050 Zurich, Switzerland, January 2011.

[19] Technical Sheet of 135W/ 125W NS-F135G5/NS-F125G5 Amorphous Silicon/Microcrystalline Silicon Sharp Middle East Fze (SMEF).

[20] Technical Sheet of CdTe panel with Thin Film Solar Module Cx3-Constructor CALYXO.

[21] Technical Sheet of Solar Panel POWERMAX, No. 9000222, Data Valid for Modules Produced on/after January 1, 2013 Starting with Serial Number: AVANCISX130101XXXX, Edition: January 2013.

[22] J.A. Ramos Hernanz, J.M. Lopez Guede, I. Zamora Belver, P. Eguia Lopez, E. Zulueta, O. Barambones, F. Oterino Echavarri, "Modelling of a Photovoltaic Panel Based on their Actual Measurements", International Journal on Technical and Physical Problems of Engineering (IJTPE), Issue 2, Vol. 6, No. 4, pp. 37-41, December 2014.

[23] J.A. Ramos Hernanz, J.J. Campayo, J. Larranaga, E. Zulueta, O. Barambones, J. Motrico, U. Fernandez Gamiz, I. Zamora, "Two Photovoltaic Cell Simulation Models in Matlab/Simulink", International Journal on Technical and Physical Problems of Engineering (IJTPE), Issue 10, Vol. 4, No. 1, pp. 45-51, March 2012.

BIOGRAPHIES

Hicham Idadoub was born in Agadir, Morocco, in 1988. He received the engineering degree in Mechatronic Engineering from National School of Applied Sciences (ENSA), Abdelmalek Essaadi University, Tetouan, Morocco in 2013. He is currently studying for his Ph.D. degree in ENSA, Ibn Zohr University, Agadir, Morocco. His current research interests include active modeling and control of electronic converters, photovoltaic energy systems, distributed generation, and artificial intelligence applied to power electronics.

Mustapha Kourchi was born in 1971 in Morocco. He received the engineering degree in Electrical Engineering from Higher Normal School of Technology (ENSET), Rabat, Morocco in 1994, Graduate Diploma in Energetic from National School of Applied Sciences (ENSA),

Agadir, Morocco in 2004, and Ph.D. degree in Automatic Control in 2011 from the Ibn Zohr university, Agadir, Morocco. His doctoral investigations took place in the Research Team on Intelligent Systems and Energy Management (ERSIME) Agadir, Morocco. He is a Professor and researcher at the Ibn Zohr University, Agadir, Morocco. He coordinates several research projects with private companies and public institutions in Morocco. His research, in the context of national doctoral thesis focuses on the thematic of renewable energies.

Mohamed Ajaamoum was born in . He received a Graduate Diploma in Software Engineering and Computer Networks from the National School of Applied Sciences (ENSA), Agadir, Morocco. His doctoral studies is taking place at the Research Team in Advanced Technologies and Engineering of Renewable Energies (ERTAIER), Agadir, Morocco in 1971. He is a Professor of higher education at High School of Technologies of Guelmim (ESTG) and Ibn Zohr University, Agadir, Morocco. He was Assistant Professeur in Electrical Engineering at Faculty of Science, Ibn Zohr University, Agadir, Morocco. His areas of research include optimization techniques, renewable energies. He is a member of Laboratory of Engineering Sciences and Energy Management (LASIME) of High School of Technologies (ESTA), Agadir, Morocco. Research Team: Intelligent Systems and Energy Management: ERSIME.

Driss Yousfi was born in Oujda, Morocco in 1970. He received the B.S. and M.S. degrees in Electrical Engineering from Fes University, Morocco in 1994 and 1996, respectively. He received the Ph.D. degree in Electrical Engineering from Oujda University, Morocco in 2001. In 1996, he was associated with the laboratory (LESSI) in Fes University when he worked on 'Adaptive Control of Interconnected Systems'. He is an Assistant Professor of Power Electronics and Electric Drives at Marrakech University, Morocco. His current area of interest is related to the innovative control strategies for ac drives, especially PM motor drives, DTC and sensor less control. He is a member of the IEEE Industry Applications, IEEE Industrial Electronics, and IEEE Power Electronics Societies.

Azeddine Rachdy received D.E.A. and Ph.D. degrees in Electronics from University of Sciences and Techniques of Languedoc, Montpellier, France in 1985 and 1988, respectively. He is a Full Professor and researcher at High School of Technology, University Ibn Zohr, Agadir, Morocco. He directs research work on renewable energies. He studied the properties of oxide thin films: SiO_2, Al_2O_3, MgO and their binary alliances on antimonides: GaSb degenerate and Ga_0, $_{96}Al_0$, $_{04}Sb$ in Integrated Energy Teaching Engineering, High School of Technology, Agadir, Morocco.